Journal of Robotics and Control (JRC)
Volume 6, Issue 3, 2025
ISSN: 2715-5072, DOI: 10.18196/jrc.v6i3.24721 

# Comparative Study of Linear and Nonlinear Controllers for DFIG-Based Wind Power Systems Under Different Operating Conditions

Achraf El Ouali [1], Yassine Lakhal [2], Mohamed Benchagra [3], Hamid Chojaa [4], Mohamed Vall O. Mohamed [5], Alfian Maarif [6], Mahmoud A. Mossa [7*]
[1, 2, 3] Department Team of Engineering and Applied Physics Higher School of Technology of Beni Mellal, Morocco
[4] Industrial Technologies and Services Laboratory, Higher School of Technology, Sidi Mohamed Ben Abdellah University, Fez 30000, Morocco
[5] Department of Computer Engineering and Networks, College of Computer and Information Sciences, Jouf University, Sakaka 75471, Saudi Arabia
[6] Department of Electrical Engineering, Universitas Ahmad Dahlan, Yogyakarta, Indonesia
[7] Electrical Engineering Department, Faculty of Engineering, Minia University, Minia 61111, Egypt
Emails: [1] elouali.hraf@gmail.com, [2] lakhal.yassine.doc@gmail.com, [3] m.benchagra@gmail.com, [4] hamid.chojaa@usmba.ac.ma, [5] medvall@ju.edu.sa, [6] alfianmaarif@ee.uad.ac.id, [7] mahmoud_a_mossa@mu.edu.eg
*Corresponding Author

*Abstract*—**When doubly-fed induction generators (DFIGs) powered by wind energy are connected to the grid, unstable grid voltage causes distortion in the control of statoric active and reactive powers, especially if the controller uses this grid value for efficiency control, as well as parameter variation. Accordingly, this study focuses on evaluating the DFIG dynamics using different control topologies. The study presents a comparative analysis of linear and nonlinear control techniques for the DFIG, including both classical and robust controllers. A voltage converter based on Pulse Width Modulation (PWM) is employed to interface with the rotor, enabling independent control of active and reactive powers. Active and reactive powers are controlled using a linear proportional-integral (PI) controller and two types of nonlinear controllers: Backstepping (BSC) and Sliding Mode (SMC). This comparative study seeks to identify the most effective controller for tracking power reference, response to speed variations, sensitivity to external disturbances, and resilience against fluctuations in machine parameters. Three sets of evaluation tests are considered: normal operation with constant rotational speed while varying power references, robustness test under DFIG's parameters variation and rotor speed perturbation. The obtained results confirm the superiority of the nonlinear BSC and SMC approaches in comparison with the FOC, giving the BSC more priority than the SMC.**

***Keywords—Doubly-Fed Induction Generator (DFIG); Wind Energy; Linear-Nonlinear Controller; Proportional-Integral (PI); Sliding Mode (SMC); Backstepping (BSC); Robustness.***

## I. Introduction

The world is moving to mainstream wind energy, especially the ones that are based on the doubly-fed induction generator (DFIG). It is the expected renewable source of electricity generation in the future, due to its high energy conversion efficiency from variable-speed operation and relatively low-cost power electronic converters [1]-[9]. The performance control of DFIG for producing electrical energy depends on controllers that simplify system behavior using linearized transfer functions. One of the most common methods is vector control, which applies field-oriented control (FOC) along with a proportional-integral (PI) controller to regulate the rotor-side converter (RSC). In fact, the equation of DFIG is naturally nonlinear and multivariable [10]-[14], [44]. The use of the PI controller, based on linearized approaches, does not fully capture the system's complexity, resulting in several disturbances and variables that are not considered in the controller synthesis [1]-[15], [46]. This approach typically rests on two main assumptions: that stator flux or stator voltage remains constant [42], [45]. However, the stator flux is not always constant, especially when there is a sudden change in stator voltage under grid faults [43], [46]. Additionally, DFIG parameters can vary due to natural phenomena, such as temperature effects, saturation, and skin effect.; so, the PI controller be less effective [16]. The main challenge when adopting linear regulators such as PI or PID is the coefficients tuning process due to the dependency on the system's model. Another shortage is the slow dynamics due to the inheritance delay in the operation mechanism of these controllers. Furthermore, the system's complexity adds more to its limitations, specifically due to the need for multiple co-ordinates transformation systems.

To improve control performance, many studies [29], [30], [35]-[45] are turning to another type of control called nonlinear control, which solves the limitations of the PI controller. Nonlinear control methods take into account the full set of system equations without relying on linearized transfer functions, and they focus on ensuring stability through approaches such as the Lyapunov-based sliding mode and Backstepping methods [19], [48], especially in terms of effectiveness and robustness. The improvement in the performance under these types of controllers comes from the way by which they provide the action; for example, in BSC, the system is bisected into different sub-systems and the stability of each is investigated then gathered to derive the overall response. This procedure enhances the system stability and improves the system robustness as well. Alternatively, in SMC, the robustness is inherently ensured due to the use of hysteresis envelope for the resultant variables' deviation. Of course, there are different functions that can be adopted to accomplish this task like Sat, Sigmoid and signum functions. To provide more detailed insights on the differences between the classic linear and recent nonlinear controllers, this article presents a comparative study of three controllers: PI, SMC, and BSC, under a variety of conditions, including changes in DFIG parameters, wind turbine speed variations, and grid voltage fluctuations. In this study, we focus on managing the active and reactive power of DFIG using the rotor-side converter (RSC), which is connected to a Pulse Width Modulation (PWM) system. This approach will help in determining which controller is the most effective and responsive under these different variables. The judgement is measured in terms of the fast dynamics, high robustness to system's disturbances and system's simplicity. Wind energy conversion system involving DFIG shown in Fig. 1.

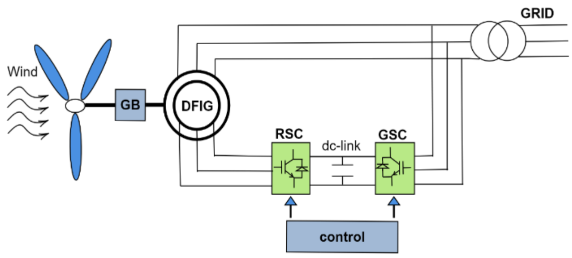


Fig. 1. Wind energy conversion system involving DFIG

First, we present the mathematical modeling of the DFIG generator, emphasizing its active and reactive powers. Then, we will discuss the control synthesis for three regulators: the linear PI, Backstepping (BSC), and robust Sliding Mode Control (SMC), with a focus on power reference tracking, responses to sudden speed changes, sensitivity to disturbances, and robustness against unbalanced grid voltage and variations in machine parameters. Finally, we analyze the results using MATLAB/SIMULINK software.

## II. Doubly Fed Induction Generator Modelling

The model Park frame (d-q co-ordinates) of DFIG may be represented using the equations for stator and rotor voltages and flux components as follows [17]-[28]:

$$\begin{cases} V_{sd} = R_s i_{sd} + \dfrac{d}{dt}\phi_{sd} - \omega_s \phi_{sq} \\ V_{sq} = R_s i_{sq} + \dfrac{d}{dt}\phi_{sq} + \omega_s \phi_{sd} \\ V_{rd} = R_r i_{rd} + \dfrac{d}{dt}\phi_{rd} - (\omega_s - \omega_r)\phi_{rq} \\ V_{rq} = R_r i_{rq} + \dfrac{d}{dt}\phi_{rq} + (\omega_s - \omega_r)\phi_{rd} \end{cases} \tag{1}$$

$$\begin{cases} \phi_{sd} = L_s i_{sd} + M i_{rd} \\ \phi_{sq} = L_s i_{sq} + M i_{rq} \\ \phi_{rd} = L_r i_{rd} + M i_{sd} \\ \phi_{sq} = L_r i_{rq} + M i_{sq} \end{cases} \tag{2}$$

The stator active and reactive powers are written:

$$\begin{cases} P_s = \dfrac{3}{2}\left(V_{sd} i_{sd} + V_{sq} i_{sq}\right) \\ Q_s = \dfrac{3}{2}\left(V_{sq} i_{sd} - V_{sd} i_{sq}\right) \end{cases} \tag{3}$$

The relationship between the stator and rotor pulsations is given by the following equation:

$$\omega_r = \omega_s - p.\Omega_g \tag{4}$$

## III. Linear Control Strategy for DFIG Systems

To apply vector control for stator active and reactive power, we use a d-q reference frame that is synchronized with the stator flux [19]-[21]. By aligning the flux vector along the d-axis, we obtain: $\emptyset_{sd} = \Psi_s$ and $\emptyset_{sq} = 0$. Assuming the electrical grid is stable, characterized by a simple voltage $V_s$, resulting in a stator flux $\Psi_s$ constant. Additionally, neglecting the stator resistance per phase (i.e. due to the high voltage operating ranges in case of DFIG) serves as a reasonable approximation for medium and high-power machines used in wind energy conversion systems, we get. $V_{sq} = 0$ and $V_{sd} = V_s = \omega_s \Psi_s$. Thus, the active and reactive power transferred between the DFIG stator, and the grid may be represented in terms of rotor currents as follows [24], [25]:

$$\begin{cases} P_s = -\dfrac{3}{2} V_s \dfrac{M}{L_s} i_{rq} \\ Q_s = \dfrac{3}{2}\left(V_s \dfrac{\Psi_s}{L_s} - V_s \dfrac{M}{L_s} i_{rd}\right) \end{cases} \tag{5}$$

The rotor voltages can be expressed by:

$$\begin{cases} V_{rd} = R_r i_{rd} + \sigma L_r \dfrac{d}{dt} i_{rd} - g\omega_s \sigma L_r i_{rq} \\ V_{rq} = R_r i_{rq} + \sigma L_r \dfrac{d}{dt} i_{rq} + g\omega_s \sigma L_r i_{rd} + g\dfrac{M V_s}{L_s} \end{cases} \tag{6}$$

Where $\sigma = 1 - \frac{M^2}{L_s L_r}$ is the leakage factor, the generator slip is, $g = (\omega_s - \omega_r)/\omega_s$.

Note (6) that the currents and the rotor voltages are bound by a first-order transfer function. We can correctly control the thing after having extracted the relationship of reference current with the stator power by using (5):

$$\begin{cases} i_{rd}^* = \dfrac{-L_s}{M V_s}\left(Q_s^* - \dfrac{{V_s}^2}{L_s \omega_s}\right) \\ i_{rq}^* = \dfrac{-L_s}{M V_s} P_s^* \end{cases} \tag{7}$$

### A. *Synthesis of Control Loop Current*

To determine the most suitable parameters for the PI rotor current regulators, the transfer function that relates the rotor current (d-q) components as inputs and rotor voltages as outputs should be initially derived. To accomplish this, the rotor voltage equations in d-q frame (Eq. (6)) are utilized. Fig. 2 shows the closed loop control system that represents this process.

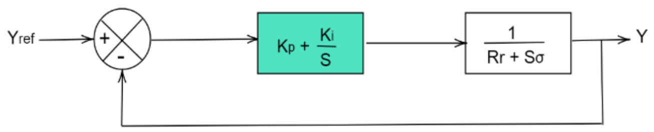


Fig. 2. Regulated by PI system

As stated earlier, the transfer function is associated with the current regulators (PI) and is determined by $(K_p + K_i/S)$ Fig.3. The open-loop transfer function (OLTF) and regulator are represented as follows:

$$OLTF = \frac{(S + \frac{K_i}{K_p})}{S/K_p} \frac{\frac{1}{\sigma}}{(S + \frac{R_r}{\sigma})} \tag{8}$$

By using compensation method to eliminate the zero a pole of the transfer function, such as:

$$\frac{K_i}{K_p} = \frac{R_r}{\sigma} \tag{9}$$

The closed loop transfer function (CLTF) is expressed by:

$$CLTF = \frac{K_p}{S\sigma} \tag{10}$$

The closed-loop transfer function (CLTF) is then formulated as:

$$CLTF = \frac{1}{1 + \tau.S} \tag{11}$$

Where $\tau = \frac{\sigma}{K_p}$

This parameter reflects the system's response time, which is around 10 ms. This duration is well-suited for our application, as reducing it further could result in significant transient overshoots. The coefficients $K_p$ and $K_i$ are then derived based on the response time and machine parameters.

$$\begin{cases} K_p = \sigma/\tau \\ K_i = R_r/\tau \end{cases} \tag{12}$$

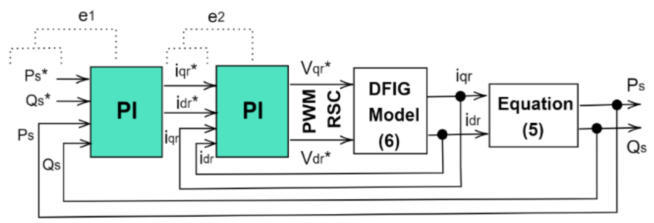


Fig. 3. Block diagram of the DFIG for indirect power control loop closed by PI.

*B. Synthesis of Control Loop Power*

Substituting (7), the expression of the current, in (6). Note that the powers and tensions are bound by a first-order transfer function.

$$\begin{cases} V_{rd} = (R_r + \sigma S).\left[\frac{-L_s}{MV_s} Q_s + \frac{V_s}{Mw_s}\right] - \omega_g \sigma i_{rq} \\ V_{rq} = (R_r + \sigma S).\left[\frac{-L_s}{MV_s} P_s\right] + \omega_g \sigma i_{rd} + g\frac{MV_s}{L_s} \end{cases} \tag{13}$$

$$OLTF = \frac{(S + \frac{K_i}{K_p})}{S/K_p} \frac{\frac{MV_s}{L_s \sigma}}{(S + \frac{R_r}{\sigma})} \tag{14}$$

$$\begin{cases} K_p = \sigma L_s/\tau_1 MV_s \\ K_i = L_s R_r/\tau_1 MV_s \end{cases} \tag{15}$$

To determine the controller coefficients for each axis, we do a control arbitrarily must that response time $\tau_1$ corresponds to the response time of the RP and RQ regulators must be shorter than the response time $\tau$ associated with the RI regulators: $\tau_1 < \tau$.

## IV. THE STRATEGY OF NON-LINEAR CONTROL OF DFIG

*A. Backstepping Controller Synthesis*

In 1990, Krstic, Kanellakopoulos, and Kokotovic discovered the backstepping strategy [29]-[32] are based on Comprehensive stability control systems, it is a method for synthesis of recursive, Backstepping is a nonlinear control approach founded on the Lyapunov theorem. Its main advantage over other techniques lies in its design flexibility [44]-[46]. The deviations between the reference values and the measured signals of stator active and reactive powers are expressed as follows [34], [52]-[54]. Block diagrams for DFIG control by Backstepping shown in Fig. 4. Block diagram for control of the DFIG by sliding mode Fig. 5.

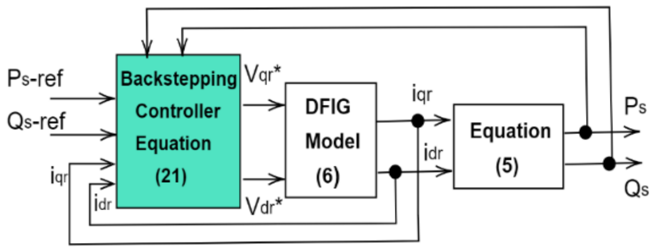


Fig. 4. Block diagrams for DFIG control by Backstepping

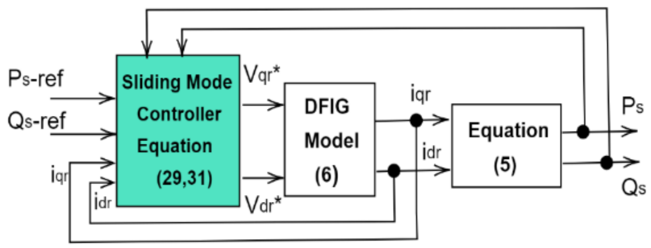


Fig. 5. Block diagram for control of the DFIG by Sliding mode

$$\begin{cases} e_1 = P_s^{ref} - P_s \\ e_2 = Q_s^{ref} - Q_s \end{cases} \tag{16}$$

Their derivates given as:

$$\begin{cases} \dot{e}_1 = \dot{P}_s^{ref} + \frac{V_s.M}{\sigma.L_r.L_s}\left(V_{rq} - R_r.i_{rq} - \sigma.L_r.\omega_r.i_{rd} + g.\frac{M.V_s}{\omega_s.L_s}\right) \\ \dot{e}_2 = \dot{Q}_s^{ref} + \frac{V_s.M}{\sigma.L_r.L_s}\left(V_{rd} - R_r.i_{rd} + \sigma.L_r.\omega_r.i_{rq}\right) \end{cases} \tag{17}$$

We define the Lyapunov function by:

$$\begin{cases} V_{(e_1)} = \frac{1}{2} e_1^2 \\ V_{(e_1,e_2)} = \frac{1}{2} e_1^2 + \frac{1}{2} e_2^2 \end{cases} \tag{18}$$

The derivative of each Lyapunov function of the error is written as follows:

$$\begin{cases} \dot{V}_{(e_1)} = e_1.\dot{e}_1 = e_1.\left(\dot{P}_s^{ref} + \frac{V_s.M}{\sigma.L_r.L_s}\left(V_{rq} - R_r.i_{rq} - \sigma.L_r.\omega_r.i_{rd} + g.\frac{M.V_s}{\omega_s.L_s}\right)\right) \\ \dot{V}_{(e_2)} = e_1.\dot{e}_1 + e_2.\dot{e}_2 = -K_1.e_1^2 + e_2\left(\dot{Q}_s^{ref} + \frac{V_s.M}{\sigma.L_r.L_s}\begin{pmatrix} V_{rd} - R_r.i_{rd} \\ +\sigma L_r.\omega_r.i_{rq} \end{pmatrix}\right) \end{cases} \quad (19)$$

The control voltages are selected as follows:

$$\begin{cases} V_{rq}^{ref} = -\frac{\sigma.L_s.L_r}{V_s.M}.\dot{P}_s^{ref} + R_r i_{rd} + \omega_r.\sigma.L_r.i_{rd} - g.\frac{M.V_s}{\omega_s.L_s} - \frac{\sigma.L_s.L_r}{V_s.M}.K_{e_1}.e_1 \\ V_{rd}^{ref} = -\frac{\sigma.L_s.L_r}{V_s.M}.\dot{Q}_s^{ref} + R_r i_{rd} - \omega_r.\sigma.L_r.i_{rq} - \frac{\sigma.L_s.L_r}{V_s.M}.K_{e_2}.e_2 \end{cases} \quad (20)$$

Where: $K_{e_1}$ and $K_{e_2}$ are positives constants.

## B. *Synthesis of Sliding Mode Controller*

The Sliding mode control operates by guiding the state trajectory back to the sliding surface and ensuring it moves along it at a dynamic equilibrium point [33]-[36]. For a nonlinear system described as follows:

$$\dot{x} = f(x,t) + g(x,t)U(x,t)\,;\; x \in R^n\,;\; U \in R \quad (21)$$

Where $f(x,t), g(x,t)$ These are two continuous and uncertain nonlinear functions, assumed to be bounded. We utilize the general equation proposed by J.J. Slotine and Li to define the slip surface, expressed as:

$$S(x) = \left(\frac{d}{dt} + \lambda_s\right)^{n-1} e(x);\; e(x) = x^d - x^* \quad (22)$$

Here, e(x) denotes the difference between the desired signal $x^d$ and the reference $x^*$. $\lambda_s$ and n represent the positive coefficient and the relative degree, respectively. The controller's structure consists of two parts: the first for exact linearization, and the second for stabilization. This is especially important in sliding mode control, where it helps reject external disturbances. Accordingly:

$$V = V^{eq} + V^n \quad (23)$$

$V^{eq}$ represents the equivalent control as proposed by Filipov and Utkin. It is used to maintain state on sliding surface $V = 0$ It is determined by recognizing that the system's behavior during the sliding mode is characterized by:

$$\dot{S(x)} = 0 \quad (24)$$

$V^n$ For satisfy the condition of convergence $S(x).\dot{S(x)} \leq 0$ It defines the system's behavior during the convergence phase, ensuring that the controlled variable is attracted to the sliding surface, and is expressed as:

$$\dot{S(x)} = V^n \quad (25)$$

In our study, we select the error mode surfaces using $n = 1$, allowing us to formulate the following expression:

$$\begin{cases} S(P_s) = P_s^{ref} - P_s \\ S(Q_s) = Q_s^{ref} - Q_s \end{cases} \quad (26)$$

By differentiating the surfaces and substituting the terms for the powers Ps and Qs (Eq. (5)) Next, we derive the expressions for current and voltage from the voltage equation (Eq. (6)) the following is obtained:

$$\begin{cases} \dot{S}(P_s) = \dot{P}_s^{ref} + \frac{3}{2}.V_s.\frac{M}{L_s.L_r.\sigma}\left(V_{rq} - R_r.i_{rq} - g.\omega_s.\sigma.L_r.i_{rd} + g.\frac{M.V_s}{\omega_s.L_s}\right) \\ \dot{S}(Q_s) = (\dot{Q}_s^{ref} + \frac{3}{2}.V_s.\frac{M}{L_s.L_r.\sigma}.(V_{dr} - R_r i_{rd} + g.\omega_s.\sigma.L_r.i_{rq}) \end{cases} \quad (27)$$

Replacing $V_{rdq}$ by $\left(V_{rdq}^{eq} + V_{rdq}^n\right)$, the controls principals appears clearly in the following equations:

$$\begin{cases} \dot{S}(P_s) = \dot{P}_s^{ref} + \frac{3}{2}.V_s.\frac{M}{L_s.L_r.\sigma}.((V_{rq}^{eq} + V_{rq}^n) - R_r.i_{rq} - g.\omega_s.\sigma.L_r.i_{rd} \\ \qquad + g.\frac{L_m.V_s}{\omega_s.L_s}) \\ \dot{S}(Q_s) = (\dot{Q}_s^{ref} + \frac{3}{2}.V_s.\frac{M}{L_s.L_r.\sigma}.((V_{rd}^{eq} + V_{rd}^n) - R_r i_{rd} + g.\omega_s.\sigma.L_r.i_{rq}) \end{cases} \quad (28)$$

In the sliding mode and at steady state, the system satisfies the following:

$$\begin{cases} S(P_s) = 0, & \dot{S}(P_s) = 0, & V_{rq}^n = 0 \\ S(Q_s) = 0, & \dot{S}(Q_s) = 0, & V_{rd}^n = 0 \end{cases} \quad (29)$$

$V_{rdq}^{eq}$ can be derived from the previous equations and are expressed as:

$$\begin{cases} V_{rq}^{eq} = -\frac{2}{3}.\frac{\sigma.L_s.L_r}{V_s.M}.\dot{P}_s^{ref} + R_r.i_{rq} + g.\omega_s.\sigma.L_r.i_{rd} - g.\frac{M.V_s}{\omega_s.L_s} \\ V_{rd}^{eq} = -\frac{2}{3}.\frac{\sigma.L_s.L_r}{V_s.M}.\dot{Q}_s^{ref} + R_r i_{rd} - g.\omega_s.\sigma.L_r.i_{rq} \end{cases} \quad (30)$$

In the convergence mode, to ensure that: $S(P).\dot{S}(P) \leq 0$ and $S(Q).\dot{S}(Q) \leq 0$ are satisfied, we assume:

$$\begin{cases} \dot{S}(P_s) = \frac{3}{2}.V_s.\frac{M}{L_s.L_r.\sigma}.V_{rq}^n \\ \dot{S}(Q_s) = \frac{3}{2}.V_s.\frac{M}{L_s.L_r.\sigma}.V_{rd}^n \end{cases} \quad (31)$$

Therefore, the switching terms given by:

$$\begin{cases} V_{rq}^n = -K_{Vq}.(S(P_s)) \\ V_{rd}^n = -K_{Vd}.(S(Q_s)) \end{cases} \quad (32)$$

To verify the stability condition of the system, the parameters $K_{Vd}$ and $K_{Vq}$ must be positive. To minimize any potential overshoot in the voltage components $V_{rdq}$, it is typically useful to integrate voltage limiters, expressed as

$$\begin{cases} V_{rq}^{lim} = V_{rq}^{max}.sat(P_s) \\ V_{rd}^{lim} = V_{rd}^{max}.sat(Q_s) \end{cases} \quad (33)$$

# V. PERFORMANCE EVALUATION RESULTS

## A. *Tracking Tests*

The active and reactive power control response of the DFIG (6KW) using three controllers (PI, SMC, BSC) is evaluated without the PWM converter (level two) and under no perturbations or parameter variations, with the generator operating at nominal speed. The tracking test results are shown in Fig. 6, Fig. 7. As shown, it can be obviously noticed that the BSC provides the fastest dynamic with minimum deviation, and the SMC comes in the second rank. The worst dynamics are obtained under the FOC with noticeable fluctuation at starting and delayed response at transient changes. For illustration, for the active power response, the BSC takes only 0.007 sec to reach its reference, while the SMC and FOC take respectively 0.025 and 0.05 sec. Furthermore, for the reactive power response, it is very obvious that the under the FOC, high fluctuation is present due to not achieving complete decoupling between the active and reactive components. This can be inferred to that the FOC design not considered entirely all system nonlinearities like BSC and SMC approaches.

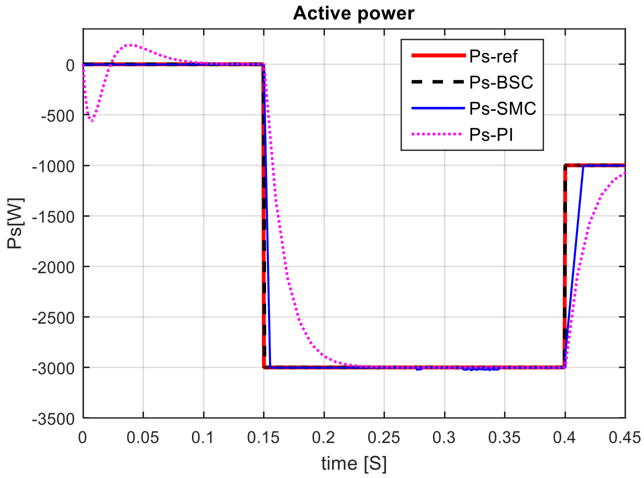


Fig. 6. Response active power (reference tracking test)

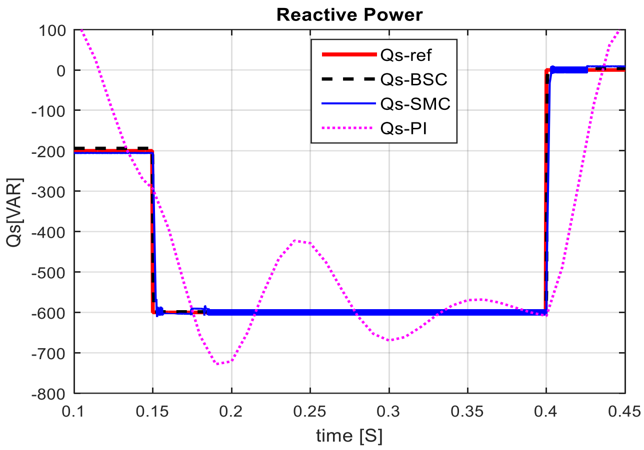


Fig. 7. Response Reactive power (reference tracking test)

## B. Robustness Tests

The robustness test examines the impact of variations in the nominal values of the generator parameters. In Fig. 8, the rotor and stator inductances, as well as the magnetizing inductance M, are increased by 50% and 20%, respectively, from their nominal values. Additionally, the rotor resistance is raised by 50% of its nominal value. It can be observed that the FOC response is the most affected one; noticeable over and under shots are present in the active power response, also there is a noticeable undershot in the reactive power value. It is also noticed that the response of the SMC is quietly delayed but without fluctuations. Alternatively, the BSC provides the most robust response without fluctuations and delay, which confirms the superiority of the BSC compared with other two techniques.

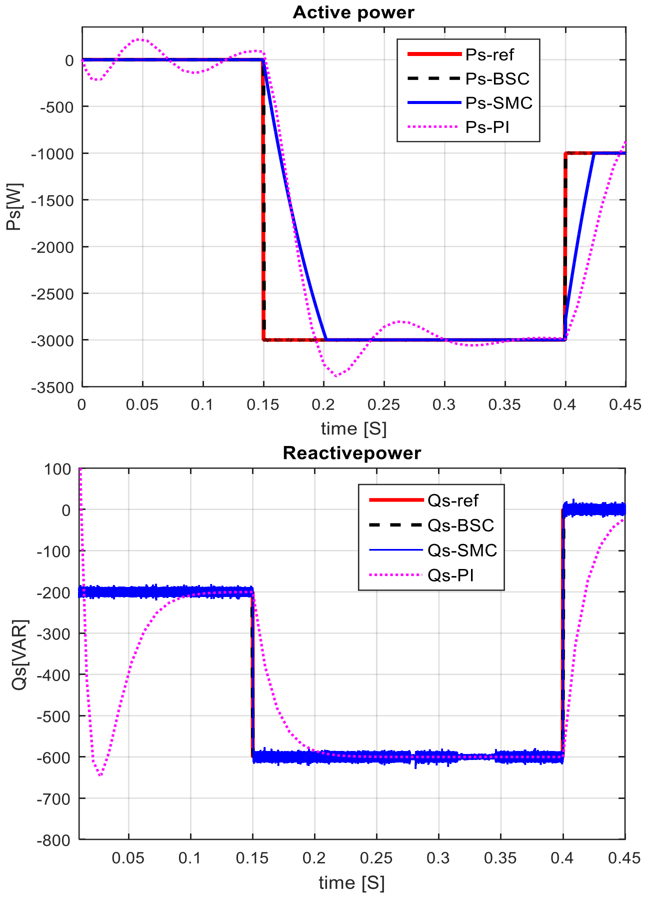


Fig. 8. Response of active and reactive power under simultaneous parameter variations $(L_r, L_s) + 50\%, M + 20\%, R_r + 50\%$

## C. Sensitivity to Perturbations

The test is concerned with evaluating the performances of the three controllers while applying a speed variation in the prime mover at instant t=3 sec. The active power is also changed from 0 to 3 Kw at instant t=2 sec. It is worth mentioning that this test adopted the usage of a PWM modulator instead of applying the reference voltages directly on the d-q model as in the previous test. The utilization of a PWM contributes in maintaining almost fixed switching frequency but contributes to add additional harmonics.

As noticed in Fig. 9, the actual active power values under the three controllers track effectively their reference signals. However, at the instant of speed variation at t=3 sec, a noticeable power fluctuation is observed under FOC. Also, there is a presence of ripples under SMC; this can be inferred to the chattering effect of SMC. Additionally, the BSC's performance exhibits the most significant response without power fluctuation or ripples.

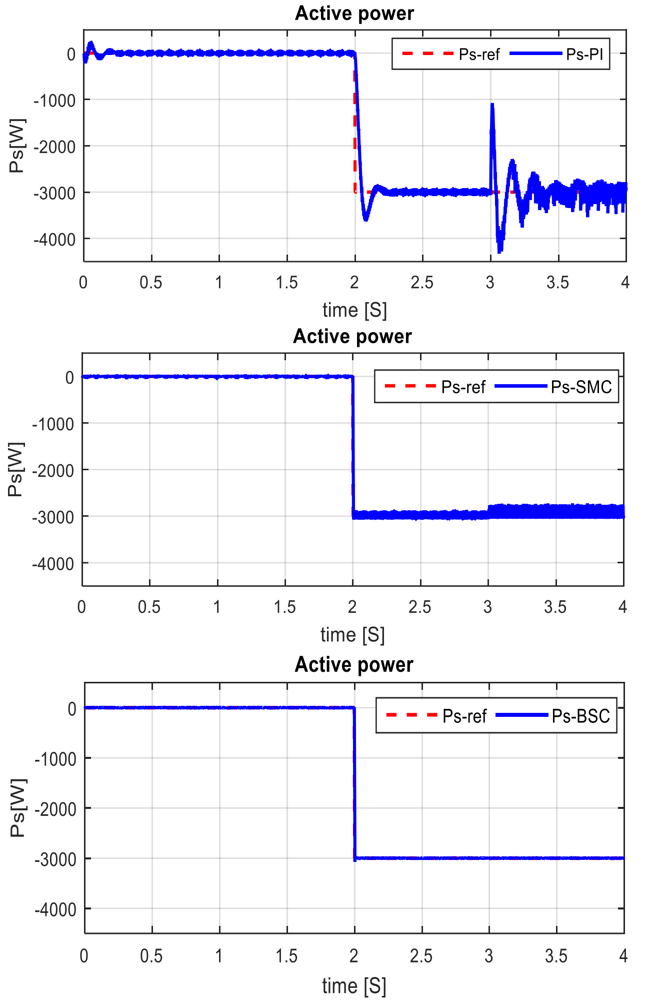


Fig. 9. Response to the active power under speed variation and increasing voltage grid when using PWM converter, (Sensitivity test)

## VI. CONCLUSION

The study presented three types of controllers after modeling the methods; namely: linear and tow non-linear controllers, PI with simplification condition, SMC with two conditions one of which is, the sign function which is a condition to ensure the convergence (Eq.31) and Lyaponov condition to ensure the stability (Eq.24); meanwhile we have BSC with one condition of Lyaponov to ensure the convergence and stability (Eq.18). These arrangements are necessary to visualize the difference in the performance of the three controllers. Firstly, we demonstrate the application of the main steps of sizing regulators namely a linear PI regulator and two nonlinear using the sliding mode and backstepping techniques for controlling the active and reactive power of DFIG. The nonlinear controllers provided better results compared with the traditional FOC. The evaluation is a accomplished by using Matlab/Simulink, The Backstepping controller demonstrates superior performance in terms of response time and reference tracking (Fig. 6, Fig. 7), and it exhibits greater robustness against DFIG parameter fluctuations compared to the standard PI and SMC controllers (Fig. 8). And finally, regarding sensitivity to perturbation, for a simulation with PWM modulated inverter and in the case of rotor speed variation. Results from simulations demonstrated the efficiency of the three types of regulators, but the Backstepping technique showed the most significant performance (Fig. 9) in the transient regimes at start-up time and variation of the power set points. The study can be further extended to evaluate the performance of other generator types after considering the theory of operation and structure of each type.

## NOMENCLATURE

| | |
|---|---|
| $V_{dc}$ | : Voltage across the DC link |
| $\Lambda$ | : Ratio of blade tip speed |
| $i_s$, $i_r$ (A) | : Current in the stator and rotor |
| $\beta$ (°) | : Blade pitch angle |
| R (m) | : Blade length |
| $\omega_s$, $\omega_r$ (rad/s) | : Angular velocity of the stator and rotor |
| $\Omega_g$ (rad/s) | : Mechanical speed of the generator |
| $\phi_s$, $\phi_r$ (Wb) | : Magnetic flux in the stator and rotor |
| $\rho$ (kg/m³) | : Air density |
| $P_s$ (W), Qs (Var) | : Active and reactive power in the stator |
| $V_s$, $V_r$ (V) | : Voltage in the stator and rotor |
| $C_p$ | : Power coefficient |
| $P_t$ (W) | : Wind turbine power output |
| V (m/s) | : Wind speed |
| P | : Number of pole pairs |
| BSC | : Backstepping control system |
| SMC | : Sliding mode control |
| RSC | : Converter for the rotor side |
| $R_s$, $R_r$ ($\Omega$) | : Stator and rotor winding resistances |
| $L_s$, $L_r$ (H) | : Stator and rotor winding inductances |
| M (H) | : Mutual inductance |

## APPENDIX

**Parameters of DFIG**

| | |
|---|---|
| Pn | = 5 KW, |
| Number of pole pairs p | = 3, |
| Nominal speed wr | = 320rad/s, |
| Grid voltage Vs-fs | = 220/380 v-50 Hz, |
| Stator resistance Rs | = 0.095$\Omega$, |
| Rotor resistance Rr | = 1.8$\Omega$, |
| Stator inductance Ls | = 0.094 H, |
| Rotor inductance Lr | = 0.088 H, |
| Stator-rotor mutual inductance M | = 0.082 H. |

## REFERENCES

[1] B. Yang, L. Jiang, L. Wang, W. Yao, and Q. Wu, “Nonlinear maximum power point tracking control and modal analysis of DFIG based wind turbine,” *International Journal of Electrical Power &*

*Energy Systems*, vol. 74, pp. 429-436, 2016, doi: 10.1016/j.ijepes.2015.07.036.

[2] M. A. Mossa, H. Echeikh, and A. Iqbal, "Enhanced control technique for a sensor-less wind driven doubly fed induction generator for energy conversion purpose," *Energy Reports*, vol. 7, pp. 5815-5833, 2021, doi: 10.1016/j.egyr.2021.08.183.

[3] M. A. Mossa, M. K. Abdelhamid, A. A. Hassan, and N. Bianchi, "Improving the Dynamic Performance of a Variable Speed DFIG for Energy Conversion Purposes Using an Effective Control System," *Processes*, vol. 10, no. 3, p. 456, 2022, doi: 10.3390/pr10030456.

[4] H. Chojaa *et al*., "Robust Control of DFIG-Based WECS Integrating an Energy Storage System With Intelligent MPPT Under a Real Wind Profile," *IEEE Access*, vol. 11, pp. 90065-90083, 2023, doi: 10.1109/ACCESS.2023.3306722.

[5] M. S. Ali, A. Sharma, T. A. Joy, and M. A. Halim, "A Comprehensive Review of Integrated Energy Management for Future Smart Energy System," *Control Systems and Optimization Letters*, vol. 2, no. 1, pp. 43-51, 2024, doi: 10.59247/csol.v2i1.77.

[6] S. D. Perkasa, A. R. Muzadi, P. Megantoro, and V. Pandi, "Audio-Based Telemetry Using HT Radios for Remote Monitoring of Renewable Energy Systems," *Control Systems and Optimization Letters*, vol. 3, no. 1, pp. 68-74, 2025, doi: 10.59247/csol.v3i1.181.

[7] F. Ahmed, A. Uzzaman, M. I. Adam, M. Islam, M. M. Rahman, and A. M. Islam, "AI-Driven Microgrid Solutions for Enhancing Energy Access and Reliability in Rural and Remote Areas: A Comprehensive Review," *Control Systems and Optimization Letters*, vol. 3, no. 1, pp. 110-116, 2025, doi: 10.59247/csol.v3i1.183.

[8] J. A. Pranto, M. M. Kadir, and M. Y. A. Khan, "A Comprehensive Study of the Importance of Materials for Renewable Energy Generation," *Control Systems and Optimization Letters*, vol. 2, no. 3, pp. 310-316, 2024, doi: 10.59247/csol.v2i3.119.

[9] M. A. Halim, M. S. Akter, S. Biswas, and M. S. Rahman, "Integration of Renewable Energy Power Plants on a Large Scale and Flexible Demand in Bangladesh's Electric Grid-A Case Study," *Control Systems and Optimization Letters*, vol. 1, no. 3, pp. 157-168, 2023, doi: 10.59247/csol.v1i3.48.

[10] T. Aziz, Z. Dodaev, M. Halim, and M. Khan, "A Review on Integration Challenges for Hybrid Energy Generation Using Algorithms," *Control Systems and Optimization Letters*, vol. 2, no. 2, pp. 162-171, 2024, doi: 10.59247/csol.v2i2.85.

[11] S. I. Khan, Z. Al Dodaev, and A. Haque, "The Integration of Renewable Energy Sources into Mechanical Systems, Focusing on Efficiency and Reliability - A Case Study," *Control Systems and Optimization Letters*, vol. 2, no. 2, pp. 172-177, 2024, doi: 10.59247/csol.v2i2.92.

[12] M. N. Hussain, K. A. Kader, M. S. Ali, A. Ullah, and Z. Al Dodaev, "An Extensive Analysis of the Significance and Difficulties of Microgrids Based on Renewable Energy in Wireless Sensor Networks," *Control Systems and Optimization Letters*, vol. 2, no. 2, pp. 178-183, 2024, doi: 10.59247/csol.v2i2.102.

[13] M. M. Mahmoud, I. Benlaloui, B. Benbouya, and N. F. Ibrahim, "Investigations on Grid-Connected DFIWGs Development and Performance Analysis with the Support of Crowbar and STATCOM," *Control Systems and Optimization Letters*, vol. 2, no. 2, pp. 191-197, 2024, doi: 10.59247/csol.v2i2.109.

[14] H. H. H. Mousa, K. Mahmoud, and M. Lehtonen, "Book Review on Hosting Capacity for Smart Power Grids, Ahmed F. Zobaa, Shady H. E. Abdel Aleem et al. Springer, 1 2020," *Control Systems and Optimization Letters*, vol. 2, no. 2, pp. 150-153, 2024, doi: 10.59247/csol.v2i2.98.

[15] J. Mohammadi, S. Vaez-Zadeh, S. Afsharnia, and E. Daryabeigi, "A Combined Vector and Direct Power Control for DFIG-Based Wind Turbines," *IEEE Transactions on Sustainable Energy*, vol. 5, no. 3, pp. 767-775, 2014, doi: 10.1109/TSTE.2014.2301675.

[16] M. A. Mossa, H. Echeikh, A. A. Z. Diab, and N. V. Quynh, "Effective Direct Power Control for a SensorLess Doubly Fed Induction Generator with a Losses Minimization Criterion," *Electronics*, vol. 9, no. 8, p. 1269, 2020, doi: 10.3390/electronics9081269.

[17] G. Abad, J. López, M. Rodríguez, L. Marroyo, and G. Iwanski, *Doubly Fed Induction Machine: Modeling and Control for Wind Energy Generation Applications*. John Wiley & Sons, 2011.

[18] M. A. Mossa and Y. S. Mohamed, "Novel Scheme for Improving the Performance of a Wind Driven Doubly Fed Induction Generator During Grid Fault," *Wind Engineering*, vol. 36, no. 3, pp. 305-334, 2012, doi: 10.1260/0309-524X.36.3.305.

[19] O. Bachir and A. F. Zoubir, "Comparative analysis of robust controller based on classical proportional-integral controller approach for power control of wind energy system," *Revue roumaine des sciences techniques Série Électrotechnique et Énergétique*, vol. 63, no. 2, pp. 210-216, 2018.

[20] M. S. Chabani, M. T. Benchouia, A. Golea, A. Y. Abdealziz, and M. A. Mossa, "A new sensor-less voltage and frequency control of stand-alone DFIG based dead-beat direct-rotor flux control-experimental validation," *ISA Transactions*, vol. 158, pp. 715-734, 2025, doi: 10.1016/j.isatra.2024.12.039.

[21] A. Loulijat, A. Hilali, M. Makhad, H. Chojaa, N. Ababssi, and M. A. Mossa, "Low-voltage ride-through capability of DFIG-based WECS improved by nonlinear backstepping controller synthesized in novel power state model," *e-Prime - Advances in Electrical Engineering, Electronics and Energy*, vol. 11, p. 100864, 2025, doi: 10.1016/j.prime.2024.100864.

[22] K. Sayed, M. Aref, M. A. Mossa, and A. G. Abokhalil, "Intelligent Control of DFIG-Based Wind Energy Conversion Systems Using Artificial Intelligence Techniques," *Energy Conversion Systems-Based Artificial Intelligence*, pp. 83-106, 2025, doi: 10.1007/978-981-96-2665-6_5.

[23] A. Chantoufi, A. Derouich, N. E. Ouanjli, S. Mahfoud, A. E. Idrissi, and M. A. Mossa, "Fuzzy Logic Speed Controller for DTC of Doubly Fed Induction Traction Motor in Electric Vehicles," *Energy Conversion Systems-Based Artificial Intelligence*, pp. 139-155, 2025, doi: 10.1007/978-981-96-2665-6_7.

[24] M. A. Mossa, T. Duc Do, A. Saad Al-Sumaiti, N. V. Quynh, and A. A. Z. Diab, "Effective Model Predictive Voltage Control for a Sensorless Doubly Fed Induction Generator," *IEEE Canadian Journal of Electrical and Computer Engineering*, vol. 44, no. 1, pp. 50-64, 2021, doi: 10.1109/ICJECE.2020.3018495.

[25] M. A. Mossa, N. E. Ouanjli, O. Gam, and O. M. Kamel, "Performance improvement of a hybrid energy system feeding an isolated load," *2022 23rd International Middle East Power Systems Conference (MEPCON)*, pp. 1-8, 2022, doi: 10.1109/MEPCON55441.2022.10021715.

[26] M. A. Mossa, O. Gam, N. Bianchi, and N. V. Quynh, "Enhanced Control and Power Management for a Renewable Energy-Based Water Pumping System," *IEEE Access*, vol. 10, pp. 36028-36056, 2022, doi: 10.1109/ACCESS.2022.3163530.

[27] M. A. Mossa, T. D. Do, H. Echeikh, and A. A. Z. Diab, "A Predictive Voltage Control Scheme For A Variable Speed Doubly Fed Induction Generator," *2021 IEEE 12th Energy Conversion Congress & Exposition - Asia (ECCE-Asia)*, pp. 1491-1497, 2021, doi: 10.1109/ECCE-Asia49820.2021.9479146.

[28] M. A. Mossa and S. Bolognani, "Predictive Power Control for a Linearized Doubly Fed Induction Generator Model," *2019 21st International Middle East Power Systems Conference (MEPCON)*, pp. 250-257, 2019, doi: 10.1109/MEPCON47431.2019.9008085.

[29] M. Krstic, I. Kanellakopoulos, and P. V. Kokotovic, "Nonlinear Design of adaptive Controllers for linear Systems, *IEEE Transactions on Automatic Control*, vol. 39, pp. 738-752, 1994, doi: 10.1109/9.286250.

[30] M. Krstic, P. V. Kokotovic, and I. Kanellakopoulos, *Nonlinear and adaptive control design*. John Wiley & Sons, 1995.

[31] M. A. Mossa, N. V. Quynh, H. Echeikh, Hamdi, and T. D. Do, "Deadbeat-Based Model Predictive Voltage Control for a Sensorless Five-Phase Induction Motor Drive," *Mathematical Problems in Engineering*, vol. 2020, no. 1, pp. 1-30, 2020, doi: 10.1155/2020/4164526.

[32] M. A. M. Basri, A. R. Husain, and K. A. Danapalasingam, "Robust Chattering Free Backstepping Sliding Mode Control Strategy for Autonomous Quadrotor Helicopter," *International Journal of Mechanical & Mechatronics Engineering IJMME-IJENS*, vol. 14, no. 03, pp. 36-44, 2014.

[33] L. Yassine, B. F. Zahra, Y. A. E. Kadi, and B. Mohammed, "The Efficiency of Fuzzy Logic Control on the Power Stabilization of Wind Turbine," *Advances in Electrical Systems and Innovative*

*Renewable Energy Techniques*, pp. 139–145, 2024, doi: 10.1007/978-3-031-49772-8_18.

[34] S. Müller, M. Deicke, and R. W. de Doncker, “Doubly Fed Induction Generator Systems for Wind Turbines: A Viable Alternative to Adjust Speed over a Wide Range at Minimal Cost,” *IEEE Industry Applications Magazine*, vol. 8, no. 3, pp. 26-33, 2002, doi: 10.1109/2943.999610.

[35] V. I. Utkin, “Sliding mode control design principles and applications to electric drives,” *IEEE Transactions on Industrial Electronics*, vol. 40, no. 1, pp. 23-36, 1993, doi: 10.1109/41.184818.

[36] M. A. Mossa, R. A. Mohamed, and A. S. Al-Sumaiti, “Performance Enhancement of a Grid Connected Wind Turbine-Based PMSG Using Effective Predictive Control Algorithm,” *IEEE Access*, vol. 13, pp. 64160-64185, 2025, doi: 10.1109/ACCESS.2025.3557194.

[37] M. A. Mossa, A. Saad Al-Sumaiti, T. Duc Do, and A. A. Zaki Diab, “Cost-Effective Predictive Flux Control for a Sensorless Doubly Fed Induction Generator,” *IEEE Access*, vol. 7, pp. 172606-172627, 2019, doi: 10.1109/ACCESS.2019.2951361.

[38] M. A. Mossa and S. Bolognani, “Effective sensorless model predictive direct torque control for a doubly fed induction machine,” *2017 Nineteenth International Middle East Power Systems Conference (MEPCON)*, pp. 1201-1207, 2017, doi: 10.1109/MEPCON.2017.8301335.

[39] M. A. Mossa and S. Bolognani, “High performance Direct Power Control for a doubly fed induction generator,” *IECON 2016 - 42nd Annual Conference of the IEEE Industrial Electronics Society*, pp. 1930-1935, 2016, doi: 10.1109/IECON.2016.7793155.

[40] S. Khadar, A. Benkhider, A. Amari, and M. A. Mossa, “A Robust DDTC Scheme Based on Artificial Neural Networks and Genetic Algorithm for Wind Power Generation,” *Energy Conversion Systems-Based Artificial Intelligence*, pp. 71-81, 2025, doi: 10.1007/978-981-96-2665-6_4.

[41] M. A. Mossa, H. Echeikh, N. El Ouanjli, and H. H. Alhelou, “Enhanced Second-Order Sliding Mode Control Technique for a Five-Phase Induction Motor,” *International Transactions on Electrical Energy Systems*, vol. 2022, no. 1, pp. 1-19, 2022, doi: 10.1155/2022/8215525.

[42] L. Xu and Y. Wang, “Dynamic Modeling and Control of DFIG-Based Wind Turbines Under Unbalanced Network Conditions,” in *IEEE Transactions on Power Systems*, vol. 22, no. 1, pp. 314-323, 2007, doi: 10.1109/TPWRS.2006.889113.

[43] I. Erlich, J. Kretschmann, S. Mueller-Engelhardt, F. Koch, and J. Fortmann, “Modeling of wind turbines based on doubly-fed induction generators for power system stability studies,” *2008 IEEE Power and Energy Society General Meeting - Conversion and Delivery of Electrical Energy in the 21st Century*, pp. 1-8, 2008, doi: 10.1109/PES.2008.4596271.

[44] Yazhou Lei, A. Mullane, G. Lightbody, and R. Yacamini, “Modeling of the wind turbine with a doubly fed induction generator for grid integration studies,” *IEEE Transactions on Energy Conversion*, vol. 21, no. 1, pp. 257-264, 2006, doi: 10.1109/TEC.2005.847958.

[45] C. Mehdipour, A. Hajizadeh, and I. Mehdipour, “Dynamic modeling and control of DFIG-based wind turbines under balanced network conditions,” *International Journal of Electrical Power & Energy Systems*, vol. 83, pp. 560-569, 2016, doi: 10.1016/j.ijepes.2016.04.046.

[46] K. D. E. Kerrouche, L. Wang, A. V. D. Bossche, A. Draou, A. Mezouar, and L. Boumediene, “Dual robust control of grid-connected dfigs-based wind-turbine-systems under unbalanced grid voltage conditions,” *Stability Control and Reliable Performance of Wind Turbines*, 2018, doi: 10.5772/intechopen.75518.

[47] J. Hu and Y. He, “Modeling and enhanced control of DFIG under unbalanced grid voltage conditions,” *Electric Power Systems Research*, vol. 79, no. 2, pp. 273-281, 2009, doi: 10.1016/j.epsr.2008.06.017.

[48] M. A. Mossa, H. Echeikh, A. Iqbal, T. D. Do, and A. S. Al-Sumaiti, “A novel sensorless control for multiphase induction motor drives based on singularly perturbed sliding mode observer-experimental validation," *Applied Sciences*, vol. 10, no. 8, p. 2776, 2020, doi: 10.3390/app10082776.

[49] M. A. Mossa and H. Echeikh, “A novel fault tolerant control approach based on backstepping controller for a five-phase induction motor drive: Experimental investigation,” *ISA Transactions*, vol. 112, pp. 373–385, 2021, doi: 10.1016/j.isatra.2020.11.031.

[50] Y. Lakhal, F. Z. Baghli, and L. E. Bakkali, “The efficiency of bond graph approach for a flexible wind turbine modeling,” *Journal of Engineering Science and Technology (JESTEC)*, vol. 12, no. 11, pp. 2990-3010, 2017.

[51] J. J. E. Slotine, W. Li, *Applied nonlinear control*, Prentice-Hall, 1998.

[52] M. A. Mossa, M. K. Abdelhamid, and A. A. Hassan, “Enhancing the Dynamic Performance of a Wind Driven Grid Connected DFIG Using an Effective Control Approach,” *2023 IEEE Conference on Power Electronics and Renewable Energy (CPERE)*, pp. 1-7, 2023, doi: 10.1109/CPERE56564.2023.10119614.

[53] M. Hussein, A. M. Mohamed, A. H. Ahmed, and A. M. Mahmoud, “Optimal predictive voltage control of a wind driven five phase PMSG system feeding an isolated load,” *e-Prime - Advances in Electrical Engineering, Electron and Energy*, vol. 9, p. 100697, 2024, doi: 10.1016/j.prime.2024.100697.

[54] M. A. Mossa, H. Echeikh, N. V. Quynh, and N. Bianchi, “Performance dynamics improvement of a hybrid wind/fuel cell/battery system for standalone operation,” *IET Renewable Power Generation*, vol. 17, no. 2, pp. 349–375, 2023, doi: 10.1049/rpg2.12603.